*Electronic Letters on Computer Vision and Image Analysis 25(2):20-38, 2026*

# Classification of Banana Leaf Disease Using Random Forest with Feature Level Fusion of LAB Color and Segmentation Area

Wulandari*, Haerunnisya Makmur*, Asmaul Husna Nasrullah*, Nur Azizah Eka Budiarti*, Satria Gunawan Zain*, Abdul Wahid*

* *Department of Computer Engineering, State University of Makassar, Makassar, Indonesia*

Received 2nd of September 2024; accepted 6th of March 2026

**Abstract**

Banana (*Musa spp.*) is a crucial commodity in tropical and subtropical regions, serving as a significant source of income for farmers and a staple food for millions of people worldwide. Due to its high export value, banana production has been increasing to meet growing market demands. However, banana plants are vulnerable to various pests and diseases, particularly on the leaves, such as Cordana, Pestalotiopsis, and Sigatoka, which can impede fruit production. Farmers typically rely on visual inspection to detect these diseases, but this method is often inaccurate due to the similarities in symptoms among these diseases. To address this challenge, digital image processing techniques combined with machine learning approaches can be utilized to enhance the accuracy and efficiency of disease detection on banana leaves. This study aims to develop a system for identifying three banana leaf diseases by employing digital image processing techniques, including threshold segmentation, color feature extraction using the LAB color space, and area analysis of segmented objects. Additionally, information fusion of extracted features was performed to improve classification accuracy. The classification results demonstrated excellent performance using Random Forest, achieving an accuracy rate of 94.75%, with precision, recall, and F1-score values of 94.37%, 93.41%, and 93.89%, respectively. The system was successfully implemented using MATLAB, enabling users to load images, perform segmentation, and easily view classification results.

*Key Words*: Random Forest, Banana Leaf, Digital Image Processing, Feature Extraction, Information Fusion, Image Classification.

## 1 Introduction

Banana (*Musa spp.*) is a crucial commodity in many tropical and subtropical countries, serving as a major source of income for farmers and a staple food for millions of people worldwide [1]. It also plays a vital role in many developing countries due to its high production, extensive trade, and significant global consumption [2]. According to the Food and Agriculture Organization (FAO), banana ranks as the highest globally produced fruit, reaching 135 million tonnes by 2022 [3]. With this substantial production, the international banana trade

Correspondence to: asmaul.husnah@unm.ac.id

Recommended for acceptance by Angel D. Sappa
https://doi.org/10.5565/rev/elcvia.1989
ELCVIA ISSN:15108-5097
Published by Computer Vision Center / Universitat Autònoma de Barcelona, Barcelona, Spain

has shown an increasing trend over the past decade, with global export volumes rising from approximately 15.5 million tonnes in 2011 to a peak of about 22.5 million tonnes in 2019 [4].

The increasing export demand for banana drives the need to boost production. However, banana plants are vulnerable to a range of pests and pathogens, including bacteria, fungi, and viruses, all of which can lead to diseases that severely affect yield and quality [5]. Among these, banana leaf diseases are particularly concerning, as the leaves play a critical role in photosynthesis, the process responsible for energy production necessary for fruit development [6]. Damage to or infection of the leaves can disrupt this process and lead to decreased fruit production.

For instance, studies have shown that Black Sigatoka infection in banana leaves can reduce fruit weight by up to 40% in severely affected plants, shorten the green life of the bananas, and alter the ripening process, ultimately impacting fruit quality and yield [7]. Black Sigatoka is also considered one of the most destructive banana diseases, with the highest control costs, resulting in over 38% yield losses in plantains and even greater losses in export bananas if effective control measures are not implemented [8].

Among the various diseases affecting bananas, leaf spot diseases such as Sigatoka, Cordana, and Pestalotiopsis are common. These diseases are caused by fungi including *Mycosphaerella*, *Cordana musae*, and *Pestalotiopsis spp.* [9]. Traditionally, farmers rely on visual inspection to identify these diseases, but this method is often inaccurate. While the diseases have different causal agents, their similar symptoms make accurate identification difficult and often require expert knowledge in disease recognition [10]. To address this challenge, technologies like digital image processing and machine learning approaches offer the potential to enhance the accuracy and efficiency of detecting foliar diseases [11].

## 2 Related Work

Several previous studies have conducted classification using image processing and machine learning algorithms, such as K-Nearest Neighbors (KNN). The first study classified the ripeness of palm fruit based on the extraction of RGB (Red, Green, and Blue) color, texture, and shape features, with the maximum accuracy obtained on each feature being 96.6%, 66%, and 73.3%, respectively [12]. Another study used the same classification method and object to classify the level of fruit ripeness based on HSV (Hue, Saturation, and Value) color features, with an average accuracy of 94.16% [13]. Another study still used KNN to classify the quality of quail eggs based on color and texture features, which were then fused into a single fused feature [14]. The results showed that information fusion improved the classification of Good, Medium, and Bad eggs by 11.11% compared to classification without information fusion, with an average accuracy of 77.78%.

In addition, other studies related to image identification and classification used different methods, such as Random Forest. The first research assessed mango quality based on external features extracted from images in the form of density, skin surface defects, and weight, achieving an accuracy of 98.3% [15]. Another study classified diseases on rice leaves, including bacterial blight, blast, tungro, and brown spot diseases, using Random Forest with a test accuracy of 97.62% and validation accuracy of 92.84% [16].

Several studies have identified and classified diseases in banana leaf plants using various methods. The first study conducted disease detection on banana leaves based on color, shape, and texture features using K-Means clustering in the segmentation process and Support Vector Machine (SVM) in the classification process with an accuracy of 85% was obtained to identify Sigatoka, Cucumber Mosaic Virus (CMV), Banana Bacterial Wilt, and Panama diseases [17]. Further research identified diseases in banana plants based on color, shape, and texture features, where Principal Component Analysis (PCA) was used to reduce the dimensions of the extracted features and KNN was used to identify diseases in banana plants [18]. The accuracy results for detecting Sigatoka, Banana Bunchy Top, Panama Wilt, and Streak Virus were 85%, 82%, 87%, and 72%, respectively.

Another study classified diseases on banana leaves in the form of Black Sigatoka, Yellow Sigatoka, and Banana Mosaic using HSV color extraction features, and classification using SVM with an accuracy of 83.33%

was obtained [19]. Furthermore, a study related to disease detection on banana leaves, namely Sigatoka, Cordana, and Pestalotiopsis, used the Inception and DenseNet methods with an accuracy of 84.73% [20]. Another research focused on detecting Panama Wilt disease on banana leaves based on changes in color and shape using the Agro Deep Learning Model (ADLM) development method, achieving an accuracy of 91.56%. This method consisted of the Convolutional Neural Network (CNN) method to identify potential signs of disease on banana leaves first, where if the probability score result obtained was high, then the specific areas of damage to the leaves were identified using the Deep Learning process [21].

The other study detected diseases on dragon fruit stems based on a combination of color and texture features using SVM and KNN methods as comparison methods [22]. The results showed that the classification model could distinguish between stem rot, smallpox, and insect sting diseases with an accuracy of 87.5% using SVM and 73.33% using KNN. However, the accuracy of disease identification on banana leaves remains low due to the limited application of digital image processing in existing studies. Methods such as segmentation, CIELAB (LAB) color feature extraction, object area for information fusion, and Random Forest classification algorithm have not been widely implemented to detect diseases on banana leaves.

Therefore, this study offers a more specific and innovative approach compared to previous research in detecting diseases on banana leaves. Earlier studies predominantly utilized color features based on RGB or HSV color spaces with algorithms such as KNN and SVM for fruit ripeness classification or plant disease detection. Additionally, some studies employed clustering methods like K-Means for disease spot segmentation and deep learning approaches based on CNN.

In contrast to previous studies, this research utilizes the CIELAB color space, which is capable of separating brightness and color information. Feature extraction using the $a^*$ component in this color space provides better differentiation between healthy green areas and red or yellow spots caused by infections on banana leaves. Additionally, this study employs information fusion between color features and segmented spot areas to enhance data representation quality, enabling more accurate and comprehensive disease detection.

The classification model employs the Random Forest algorithm, which has proven effective in several previous studies but has not been widely implemented for banana leaf disease detection. The uniqueness of this approach lies in the application of feature-level fusion between LAB color features and segmented area size features, which has not been widely explored in similar studies. By integrating threshold-based segmentation, LAB feature extraction, and feature-level information fusion, this study aims to provide a more accurate and optimal solution compared to existing methods.

This approach is expected to contribute to more precise plant disease identification and significantly improve banana leaf agricultural outcomes. A comparison between this study and previous research is summarized in Table 1.

Table 1: Comparison of Studies

| **Aspects** | **This Study** | **Previous Studies** |
|---|---|---|
| Research object | Banana leaf | Oil palm fruit [12, 13], quail eggs [14], mango fruit [15], rice leaf [16], banana leaf [17, 18, 19, 20, 21], dragon fruit stems [22] |
| Segmentation method | Thresholding with the a* component in the LAB color space | Manual [12], no segmentation [13, 19], Thresholding [14, 15, 16, 22], K-Means clustering [17, 18], Deep Learning [20, 21] |
| Feature extraction methods used | Color feature extraction (LAB components) and segmented object area | RGB color [12], HSV color [13, 19], color and texture [14, 16, 17, 22], texture [18] |

*Continued on next page*

| Aspects | This Study | Previous Studies |
|---|---|---|
| Information fusion method | Information fusion with Feature In-Feature Out (FEI-FEO) method to combine color features and object area | Information fusion with FEI-FEO method [14], Feature Fusion PCA [17] |
| Classification algorithm | Random Forest (RF) | KNN [12, 13, 14, 18], RF [15, 16], SVM [17, 19], SVM and KNN [22], DenseNet [20], CNN [21] |
| Contribution | Use a combination of LAB color features and spot area with FEI-FEO information fusion and Random Forest classification | Use conventional features such as RGB and HSV color spaces or deep learning models without applying more complex information fusion methods |

# 3 Proposed Method

The research stages consist of data collection, preprocessing, segmentation, feature extraction, information fusion, classification, evaluation, and implementation, as shown in Figure 1.

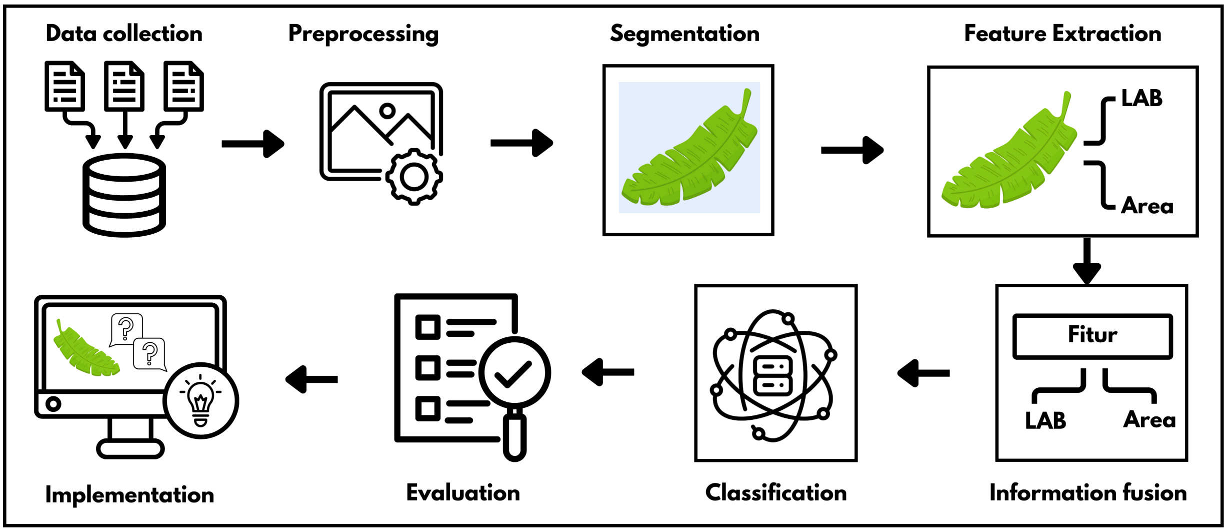


Figure 1: Research stages

## 3.1 Data Collection

The dataset used consists of banana leaf images divided into four classes. One class is healthy banana leaves, while the other three are disease-infected banana leaves. The data was collected from public sources, Kaggle, with a total of 1015 data. All images were captured in a banana plantation located at Bangabandhu Sheikh Mujibur Rahman Agricultural University, using a high-resolution rear camera [23]. The image acquisition took place in June 2021 under natural lighting conditions. To create a diverse and realistic dataset, the images were intentionally captured under varying lighting conditions and from different angles. All images showing disease symptoms were labeled by plant pathology experts to ensure classification accuracy. Details of the source and amount of data are presented in Table 2.

Table 2: Source and Amount of Data

| Source | Class | Total Data |
|---|---|---|
| [24] | Healthy | 129 |
| | Cordana | 161 |
| | Pestalotiopsis | 169 |
| | Sigatoka | 470 |
| [25] | Healthy | 86 |
| **Total** | | **1015** |

Upon collecting the dataset, it was divided into training and testing sets with a 70%:30% ratio. Each class in the dataset was split such that 70% of the data was used as training data to train the model, while the remaining 30% was used as independent test data to evaluate the model's performance. The distribution details of the training and testing sets are provided in Table 3.

Table 3: Distribution of Training and Testing Sets

| Class | Total Data | Training Set (70%) | Testing Set (30%) |
|---|---|---|---|
| Healthy | 215 | 150 | 65 |
| Cordana | 161 | 113 | 48 |
| Pestalotiopsis | 169 | 119 | 50 |
| Sigatoka | 470 | 328 | 142 |
| **Total** | **1015** | **710** | **305** |

### 3.2 Preprocessing

The preprocessing stage is the first step in image analysis, aiming to enhance image quality and prepare the image for subsequent processing. In this study, various methods were applied during preprocessing to optimize the images for further analysis. Initially, noise reduction techniques were employed, including image cropping, which served to remove extraneous elements such as background soil, sky, or objects unrelated to the banana leaf. This step helps eliminate potential distractions that could interfere with the image processing. Next, a color conversion was performed to transform the image from the RGB color space to the LAB color space. This conversion was necessary as the LAB color space provides better color differentiation, which is crucial for the accurate detection of banana leaf diseases.

### 3.3 Segmentation

Image segmentation is the process of separating a digital image into several areas based on the different characteristics of each pixel [26, 27]. In this study, segmentation was carried out to separate infected and uninfected leaf areas. Therefore, the LAB color space was used, which has three components: L (luminance), A (red to green color component), and B (yellow to blue color component).

The selection of the LAB color space is based on the ability of the A component to distinguish between red and green, which is highly relevant for detecting color differences in spots on infected leaf. On healthy leaf, the dominant color tends to be in the green spectrum, while disease spots often produce colors that lean towards the red or yellow-brown spectrum. The A component effectively captures these spectral differences with high precision, enabling more accurate separation of infected areas.

The algorithm used in the image segmentation process is binary thresholding, a simple yet effective method for separating objects from the background based on pixel intensity values. In the context of this study, thresholding was applied to distinguish disease spots on banana leaf, which exhibit a clear color contrast with the surrounding healthy areas. Binary thresholding was chosen because it provided fast and accurate results for images with high contrast between the object and the background. The flowchart of this segmentation process is shown in Figure 2.

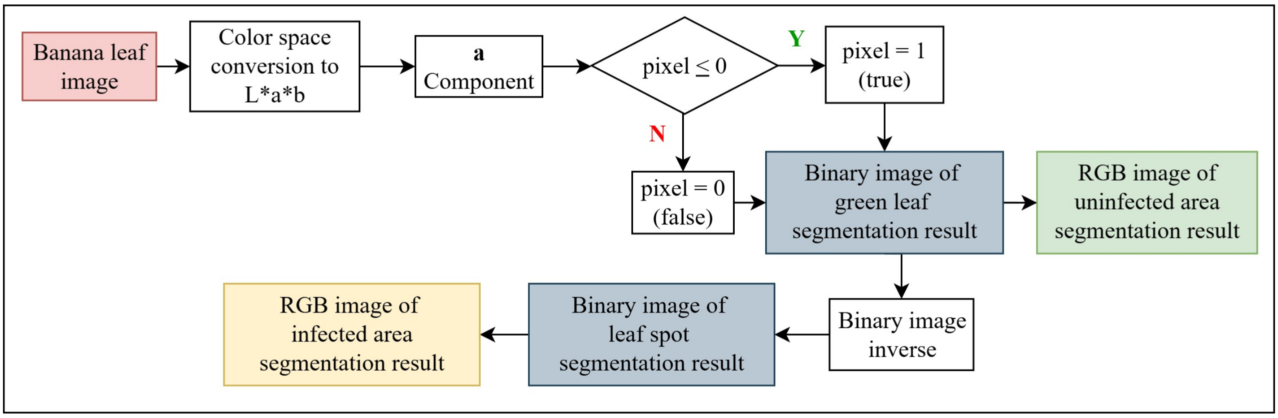


Figure 2: Flowchart of image segmentation

Based on the diagram in Figure 2, the image segmentation process only used component A because it contains red-green chromatic information, where +a* (positive) values represent red and -a* (negative) values represent green [28]. To separate the green color pixels from the red color in component A, the binary thresholding method was used with the threshold value set to 0. In general, the thresholding process to convert an image into a binary image can be represented mathematically in equation (1), where $g(x, y)$ is the binary image of the grayscale image $F(x, y)$, and $T$ is the threshold value [29].

$$g(x,y) = \begin{cases} 0 & \text{if } F(x,y) > T \\ 1 & \text{if } F(x,y) \leq T \end{cases} \tag{1}$$

The result of the thresholding process is a binary image representing the object and background areas, where pixels with a value of 1 indicate the object (green leaf area) displayed in white, while pixels with a value of 0 indicate the background displayed in black. The binary image is then inverted so that the background becomes white and the object becomes black. This segmented result is then presented back in RGB format with two variations: first, the object is shown in white on a black background, and second, the object is shown in black on a white background.

### 3.4 Feature Extraction

The feature extraction stage was performed by integrating several features, which include color and area features of the segmented image. This stage aims to extract important information from the banana leaf image to form a classification model [30]. One of the color features that can be extracted from the image is the mean value [31]. This average value of color intensity provides an overview of the distribution of colors in the image. This color feature is extracted in the LAB color space by calculating the mean using equation (2), where $M$ and $N$ are the image sizes in row and column dimensions, and $P_{i,j}$ is the color intensity value of the pixel.

$$\text{Mean} = \frac{1}{M \times N} \sum_{i=1}^{M} \sum_{j=1}^{N} P_{i,j} \tag{2}$$

Meanwhile, the area feature is used to represent the size of the object in the image by calculating the total number of segmented pixels that belong to the object. In this case, $S_{i,j}$ represents the binary segmentation image, where a value of $S_{i,j} = 1$ indicates that the pixel at position $(i, j)$ is part of the object, while $S_{i,j} = 0$ indicates that the pixel belongs to the background. By summing all the pixels, information about the object's area in pixel units is obtained, as shown in equation (3).

$$\text{Area} = \sum_{i=1}^{M} \sum_{j=1}^{N} S_{i,j} \tag{3}$$

### 3.5 Information Fusion

Information fusion is a technique used to combine multiple features into a single feature to produce more informative features [32]. The information fusion method applied in this research was Feature In-Feature Out (FEI-FEO). The FEI–FEO method in information fusion is a process in which both the input and output data are at the feature level [33]. Data from various sources are extracted into features, which are then combined to form new, more informative features. The result of this fusion is not a final decision, but rather a combined feature set that can be used for further analysis or modeling. The conceptual flow diagram of the FEI–FEO method used in this study is presented in Figure 3.

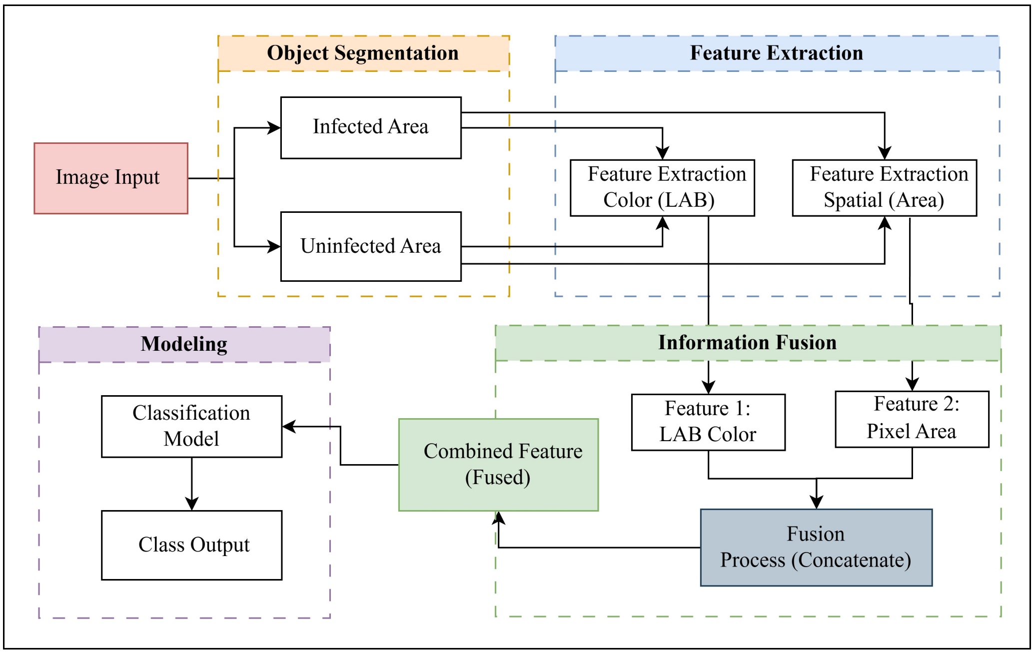


Figure 3: Flow Diagram of FEI–FEO (Feature In – Feature Out)

Based on Figure 3, the process begins with the input image, which then undergoes object segmentation to separate infected areas from non-infected areas. After segmentation, two types of feature extraction are performed: color features using the LAB color space, and spatial features such as the pixel area of the segmented object. These features are then separated into two groups: color features as Feature 1 and area size as Feature 2. The two features are then combined through a fusion process, specifically direct concatenation, resulting in a fused feature that is more representative.

This fused feature is then used as input for the Random Forest classification model, which determines the output class for banana leaf disease detection. The mathematical formulation of feature fusion is presented in equation (4), where $f$ represents the fusion function which may take the form of concatenation, weighted sum, or other methods, and $F_{m1}, F_{m2}, \ldots$ are the extracted features [34]. In this study, $F_{m1}$ represents the LAB color features, while $F_{m2}$ represents the area size feature.

$$F_{\text{Fused}} = f(F_{m1}, F_{m2}, \ldots, F_{mn}) \tag{4}$$

The FEI-FEO method has an advantage when two different features contain complementary information, allowing their combination to strengthen the data representation for detection or classification purposes. This is particularly relevant in banana leaf disease detection, where color features and spot area provide distinct yet supportive information. By combining these two features using FEI-FEO, the obtained information becomes more comprehensive and informative, enabling the model to identify clearer and more accurate patterns or characteristics in detecting diseases on banana leaf.

### 3.6 Classification

The classification stage aims to develop a model capable of identifying three common diseases affecting banana leaf. The classification process involved the use of training data, with extracted features serving as input, which were then trained using a machine learning algorithm. In this study, Random Forest was used as the classifier due to its ability to build multiple decision trees and combine their results, leading to more accurate and stable predictions. The bagging technique employed reduces variance and prevents overfitting, while effectively handling complex data. Furthermore, Random Forest also provides feature importance interpretation, which aids in further analysis.

The Random Forest model was implemented using the TreeBagger function in MATLAB, which constructed 50 decision trees through the bagging (bootstrap aggregating) technique. This number was chosen to balance computational efficiency and was based on empirical findings indicating that the performance of Random Forest models tends to stabilize after reaching 64–128 trees, meaning that a smaller number of trees can still yield representative results with lower computational cost [35]. The model was also configured with a MaxNumSplits of 100 to capture complex data patterns, with PredictorSelection set to interaction-curvature to detect interactions between predictors, and pruning was disabled to ensure that the trees remained fully utilized. Random Forest parameters, such as the number of trees (50 trees) and MaxNumSplits (100), were determined based on initial trials on the testing data, where this combination yielded the best performance compared to other configurations.

For comparison purposes, other models such as Support Vector Machine (SVM), K-Nearest Neighbors (KNN), and Artificial Neural Network (ANN) were also applied. Table 4 summarizes the parameters used in the training of each model.

Table 4: Classification model parameters

| Method | Parameters |
|---|---|
| Random Forest | Method = classification<br>MaxNumSplits = 100<br>PredictorSelection = interaction-curvature<br>Prune = off |
| SVM | KernelFunction = rbf<br>BoxConstraint = 1<br>KernelScale = auto<br>Standardize = true |
| KNN | NumNeighbors = 7<br>Distance = cityblock |

*Continued on next page*

| Method | Parameters |
|---|---|
| | DistanceWeight = inverse<br>Standardize = true |
| ANN | Hidden Layers = 10 and 5<br>Activation Function = logsig<br>Training Algorithm = trainlm<br>Epochs = 1000<br>Goal = $10^{-6}$ |

### 3.7 Evaluation

An independent test set was utilized to assess the model's performance, consisting of data that was separated and not included in the training process. The use of this independent test set ensures that the model is evaluated on unseen data, providing a more realistic assessment of its ability to generalize to new data. The performance of the classification model was evaluated using metrics such as accuracy, precision, recall, and F1-score, as shown in the confusion matrix in Table 5.

Table 5: Confusion Matrix

| | **Prediction True** | **Prediction False** |
|---|---|---|
| **Actual True** | True Positive | False Negative |
| **Actual False** | False Positive | True Negative |

The following equations calculate the accuracy, precision, recall, and F1-score values [36]:

$$\text{Accuracy} = \frac{TP + TN}{TP + FN + FP + TN} \tag{5}$$

$$\text{Precision} = \frac{TP}{TP + FP} \tag{6}$$

$$\text{Recall} = \frac{TP}{TP + FN} \tag{7}$$

$$\text{F1-Score} = \frac{2 \times \text{Precision} \times \text{Recall}}{\text{Precision} + \text{Recall}} \tag{8}$$

Precision measures the system's ability to identify positive cases from all predicted positives, recall measures the ability to identify positive cases from all actual positives, and F1-score represents the harmonic mean of precision and recall.

## 4 Result and discussion

The dataset consists of banana leaf images categorized into four classes: healthy leaves, and those infected with cordana, pestalotiopsis, or sigatoka. Figure 4 illustrates examples and the distinctive characteristics of each class. Figure 4a shows an image of a healthy banana leaf with a bright green color and aligned across its surface without any noticeable spots or discoloration. Figure 4b shows a picture of a banana leaf infected with cordana disease; there are round or oval-shaped spots with dark brown or black edges and a lighter colored center, usually light brown or grayish. Figure 4c shows that the characteristics of pestalotiopsis-infected banana leaf are brown or black spots with gray or light brown centers and often surrounded by yellow margins. These spots usually have a spotted structure in the center, a collection of fungal spores. Figure 4d shows that banana leaf infected with sigatoka disease have small yellow or light brown spots that later develop into dark brown or black stripes. In advanced stages, these spots can merge and cause a large portion of the leaf to become necrotic.

(a) Healthy (b) Cordana (c) Pestalotiopsis (d) Sigatoka

Figure 4: Banana leaf images

Among the four diseases, the most distinctive characteristics are the color and size of the disease spots on banana leaf. Therefore, during the segmentation stage, a process was conducted to identify infected and uninfected areas, which were subsequently utilized in the feature extraction stage. The segmentation process employed the LAB color space, as presented in Table 6.

Table 6: Segmentation of Banana Leaf Image in LAB Color Space

| **Image Type** | **Component L** | **Component A** | **Component B** |
|---|---|---|---|
| Grayscale | 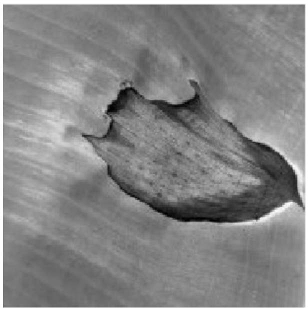 | 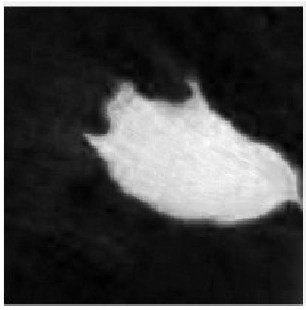 | 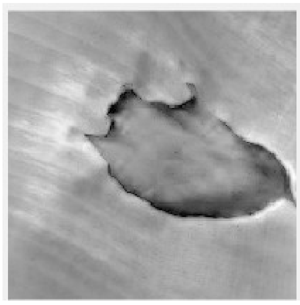 |
| Binary |  | 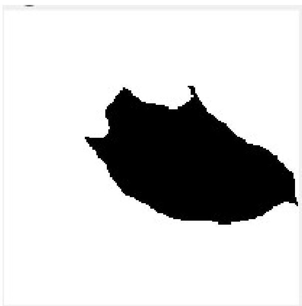 |  |

In Table 6, the segmentation process was performed using grayscale images in the LAB color space, utilizing the L, A, and B components. The binary image segmentation results for the L component demonstrated suboptimal separation of infected and uninfected areas, indicating that the L component alone was insufficient for accurately distinguishing significant color differences between these areas. This limitation arises from the L component's inability to effectively differentiate color variations.

Conversely, the A component yielded significantly more optimal segmentation results. In the grayscale image based on the A component, the distinction between infected and uninfected areas was clearly visible. The A component in the LAB color space encodes red-green color information, making it more effective in differentiating leaf color variations associated with infection. This is evident in the binary image derived from the A component, where infected and uninfected regions were distinctly segmented. The superior performance of the A component enabled more precise separation, resulting in improved segmentation quality and facilitating clearer identification of infected areas.

The segmentation results using the B component, however, were less effective. In the grayscale image derived from the B component, the distinction between infected and uninfected areas was not well-defined. The B component, which captures yellow-blue color information, was unable to effectively differentiate the relevant color variations in this context. This limitation was reflected in the binary segmentation results, where the separation of infected and uninfected areas was inferior to that achieved using the A component.

Therefore, utilizing the A component for segmentation produced a binary image in which the infected regions appeared white, while the background remained black. Figure 5 illustrates the segmentation results of both the binary image and the RGB binary image. Specifically, Figure 5a represents the segmented infected area, while Figure 5b, as its inverse, highlights the uninfected regions. The binary image presented in Figure 5a was subsequently re-rendered in RGB format, as shown in Figures 5c and 5d.

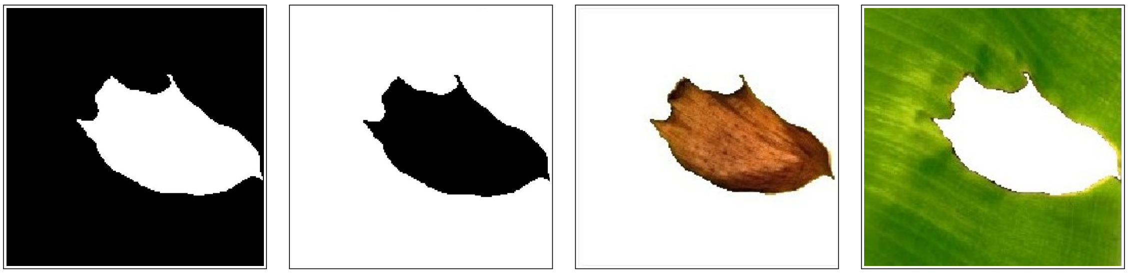

(a) Binary (b) Inverted (c) RGB Binary (d) RGB Inverted

Figure 5: Segmentation results

After completing the segmentation and morphological processing stages, the two successfully segmented objects underwent feature extraction. The feature extraction results for the training data are presented in the graph shown in Figure 6. Based on the graph in Figure 6a, the L component color feature extraction value in the infected area exhibits a higher average compared to the uninfected area. This indicates that the brightness (lightness) in the infected area is greater than in the uninfected area. Similarly, the graph in Figure 6b shows that the A component color feature extraction value has a higher average in the infected area, whereas the uninfected area displays a lower average, even reaching negative values. This is because negative values in the A component indicate a greener hue, which corresponds to the uninfected area appearing as a healthy green leaf.

Meanwhile, the graph in Figure 6c, which presents the feature extraction values for the B component, demonstrates that the uninfected area has a higher average value than the infected area. This suggests that the color of the infected leaf region is more yellow, resulting in a lower average B component value in the infected area. Additionally, the graph in Figure 6d, which illustrates the segmentation-based area feature, indicates that healthy (uninfected) leaves within data points 105–261 have a larger area compared to infected leaves. In general, a smaller infected area suggests that the infection is localized to a limited portion of the leaf, while the majority of the leaf remains healthy. Conversely, a larger infected area signifies extensive infection and severe leaf damage. The relationship between these values provides a clear representation of infection severity and leaf health distribution, serving as a key distinguishing feature in disease detection.

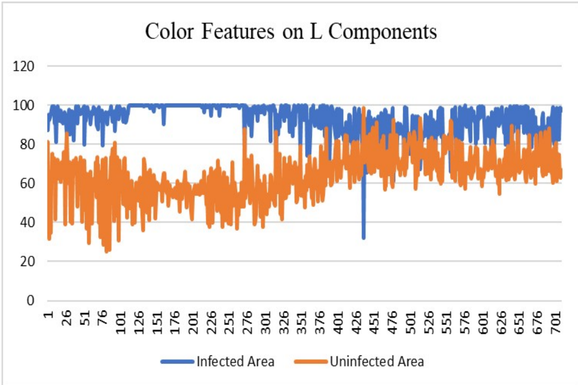


(a) Mean color intensity of L component

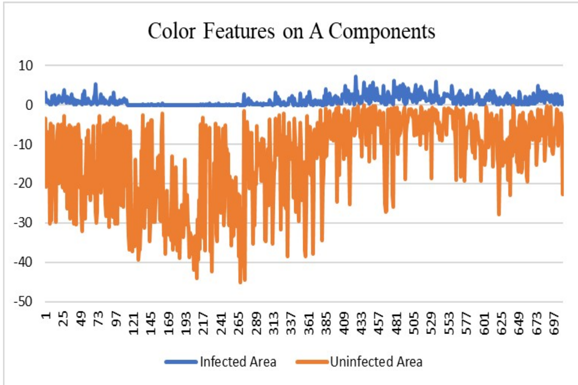


(b) Mean color intensity of A component

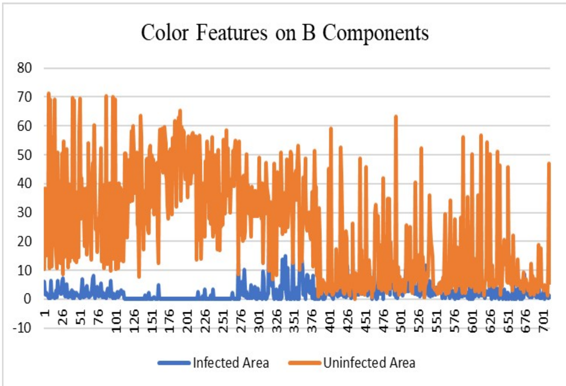


(c) Mean color intensity of B component

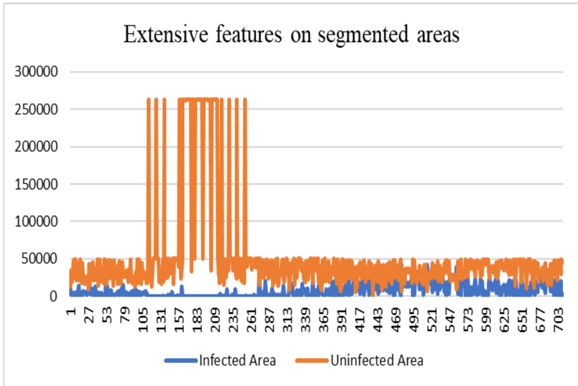


(d) Segmented object area (number of pixels)

Figure 6: Feature extraction graph

Following feature extraction, information fusion was performed to maximize classification accuracy by integrating multiple features and evaluating different color spaces. The results of the feature information fusion are presented in Table 7.

Table 7: Research scenario results using the feature information fusion

| No. | Object Segmentation | | Recall (%) | Precision (%) | F1-Score (%) | Accuracy (%) |
|---|---|---|---|---|---|---|
| | **Segmentation 1 (Infected Area)** | **Segmentation 2 (Uninfected Area)** | | | | |
| 1. | RGB Color (Without segmentation) | | 76.69 | 75.29 | 75.98 | 78.36 |
| 2. | HSV Color (Without segmentation) | | 77.17 | 78.14 | 77.65 | 80.66 |
| 3. | LAB Color (Without segmentation) | | 82.02 | 78.86 | 80.41 | 82.30 |
| 4. | RGB Color | - | 67.67 | 70.91 | 69.25 | 74.10 |
| 5. | HSV Color | - | 77.56 | 77.10 | 77.33 | 81.31 |
| 6. | LAB Color | - | 85.83 | 85.71 | 85.77 | 87.21 |
| 7. | RGB Color | RGB Color | 84.65 | 85.72 | 85.18 | 86.89 |
| 8. | HSV Color | HSV Color | 86.69 | 87.26 | 86.97 | 88.20 |
| 9. | LAB Color | LAB Color | 89.43 | 89.39 | 89.41 | 90.82 |
| 10. | LAB Color + pixel area | LAB Color | 92.70 | 91.38 | 92.04 | 92.79 |
| 11. | LAB Color | LAB Color + pixel area | 89.11 | 90.34 | 89.72 | 91.48 |
| 12. | LAB Color + pixel area | LAB Color + pixel area | 93.41 | 94.37 | 93.89 | 94.75 |

According to the classification scenario results from the feature information fusion in Table 7, it was observed that images without segmentation achieved the highest accuracy of 82.30% when using LAB color features. Meanwhile, the RGB color feature yielded an accuracy of 78.36%, while the HSV color feature achieved 80.66%. Furthermore, classification based solely on feature extraction from segmented infected areas resulted in an accuracy of 74.10% for RGB color features, 81.31% for HSV color features, and the highest accuracy of 87.21% for LAB color features.

In the subsequent scenario, where both infected and uninfected areas were segmented, the highest accuracy was obtained using the LAB color feature, reaching 90.82%. In Scenario 10, an accuracy of 92.79% was achieved by incorporating an additional feature, namely the segmented infected area size. However, when the area feature was applied to the segmented uninfected area, the accuracy slightly decreased to 91.48%. The highest accuracy was recorded in Scenario 12, where the combination of LAB color features and area features from both segmentation results yielded an accuracy of 94.75%.

The results from Scenario 12, which employed the Random Forest model, were further compared with other classification methods, including Support Vector Machine (SVM), K-Nearest Neighbors (KNN), and Artificial Neural Networks (ANN). These alternative models were selected to evaluate their performance and provide insights into how each classifier processes the same dataset. This comparison helps determine the most effective approach for this study. Table 8 summarizes the evaluation results of each classification method, utilizing consistent feature extraction techniques and data proportions.

Table 8: Comparison of classification method performance

| No. | Method | Recall | Precision | F1-Score | Accuracy |
|---|---|---|---|---|---|
| 1 | Random Forest | 93.41 | 94.37 | 93.89 | 94.75 |
| 2 | SVM | 89.82 | 88.74 | 89.28 | 90.81 |
| 3 | KNN | 90.41 | 89.17 | 89.79 | 91.15 |
| 4 | ANN | 70.76 | 71.84 | 71.30 | 75.74 |

Table 8 demonstrates that the Random Forest method outperforms the other three classification methods, achieving a recall of 93.41%, precision of 94.37%, F1-score of 93.89%, and accuracy of 94.75%. Although K-Nearest Neighbors (KNN) and Support Vector Machine (SVM) are widely used classification algorithms, their performance on this dataset is slightly lower than that of Random Forest. Meanwhile, Artificial Neural Network (ANN), which serves as the foundation of deep learning and is known for its ability to capture complex patterns, exhibited the lowest performance. This may be due to suboptimal ANN parameters or limitations in the dataset for deeper training. The superiority of Random Forest in terms of stability and higher accuracy compared to other methods is the primary reason for its selection in this scenario. The confusion matrix obtained from the classification model using the Random Forest method is presented in Table 9.

Table 9: Confusion matrix for scenario 12 using the Random Forest classification model

| Actual | Prediction | | | |
|---|---|---|---|---|
| | Healthy | Cordana | Pestalotiopsis | Sigatoka |
| **Healthy** | 61 | 0 | 2 | 2 |
| **Cordana** | 0 | 47 | 0 | 1 |
| **Pestalotiopsis** | 6 | 0 | 42 | 2 |
| **Sigatoka** | 1 | 1 | 1 | 139 |

Based on the confusion matrix from Scenario 12 in Table 9, the classification of diseases on banana leaves yielded overall positive results. However, some detection errors were observed. In the healthy class, three images were misclassified. The cordana class had only one misclassified image. The pestalotiopsis class showed more errors with seven incorrectly detected images, while the sigatoka class had six misclassified images. Several examples of misclassified banana leaf images are shown in Figure 7, where Actual indicates the true label and Predicted represents the label assigned by the classification model.

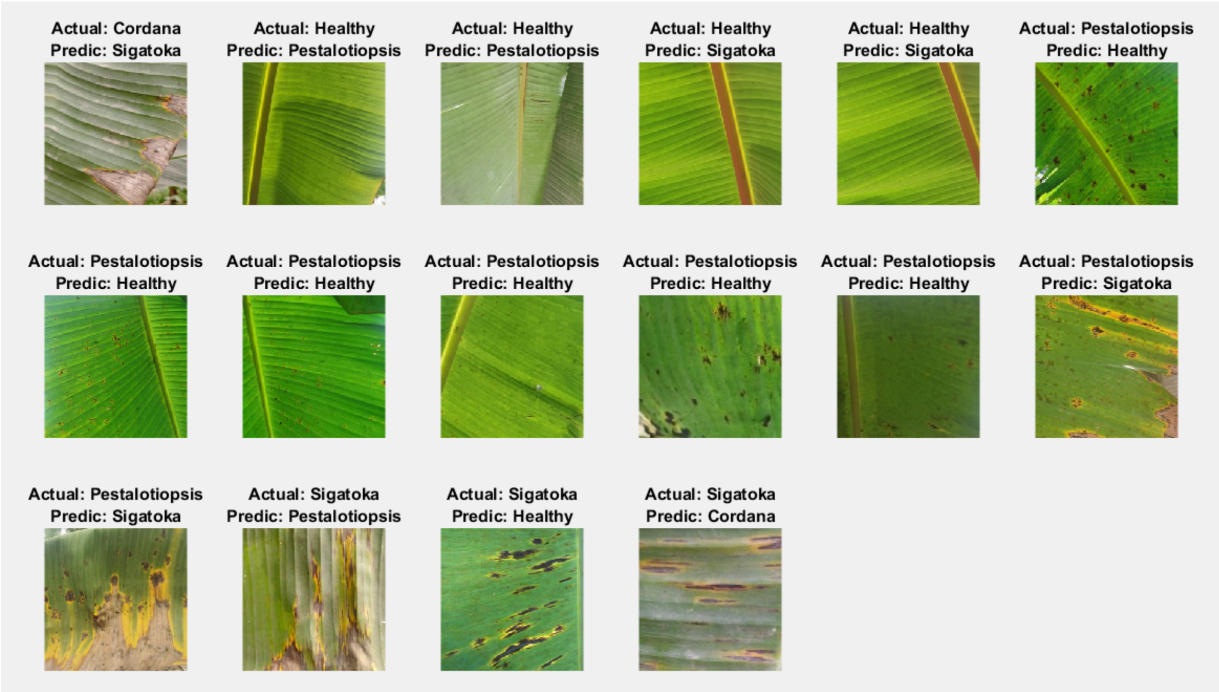


Figure 7: Examples of misclassified banana leaf images

Based on observations from Figure 7, several key factors contributing to misclassification can be identified. One of them is the visual similarity between certain diseases, such as Pestalotiopsis and Sigatoka, which both exhibit dark spots on the leaves. Under certain lighting conditions, the model struggles to distinguish between the two. Additionally, mild or early-stage infections often resemble healthy leaves due to small or low contrast spots, leading to some Pestalotiopsis infected leaves being misclassified as healthy.

Misclassification is also influenced by uneven lighting, shadows, and overlapping leaf conditions. Uneven illumination or the presence of shadows on the leaves can alter the perceived color, particularly in the $a^*$ channel of the LAB color space used for segmentation. The binary threshold set at $a^* = 0$ is relatively simple and yields good results under ideal conditions. However, this method is quite sensitive to lighting variations, as the $a^*$ values can shift significantly due to different lighting conditions, thereby affecting the segmentation outcome.

Inaccurate segmentation directly impacts the feature extraction process for both color and area. As a result, some healthy leaves that are partially covered by shadows or have prominent stems may be incorrectly detected as infected leaves. In addition, Sigatoka and Cordana are sometimes confused with one another due to their similar necrotic patterns and spot colors. This indicates that color and area features alone are not sufficient to distinguish certain types of diseases. The inclusion of additional features, such as texture or spot shape, has the potential to improve classification accuracy.

The classification model developed in Scenario 12 was subsequently applied to detect diseases in banana leaf images. This system enables users to process images, directly detect diseases, perform segmentation, and view the results via the user interface. Figure 8 illustrates the classification process, showcasing the results of four banana leaf images: Figure 8(a) depicts a healthy leaf, Figure 8(b) shows a leaf infected with Cordana, Figure 8(c) shows a leaf infected with Pestalotiopsis, and Figure 8(d) displays a leaf infected with Sigatoka.

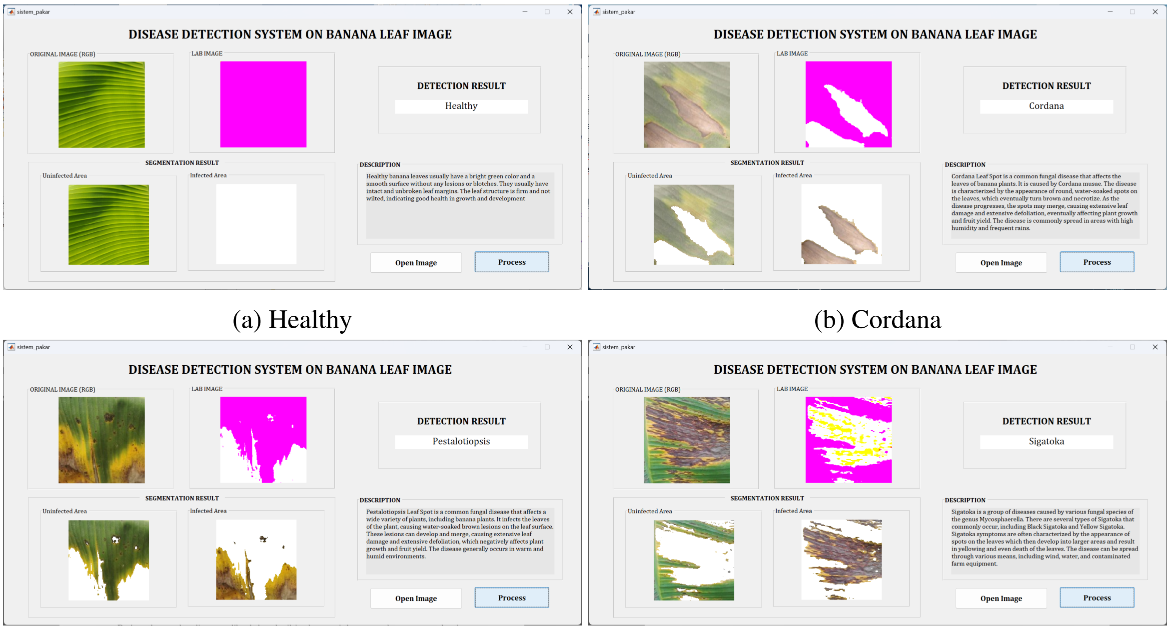


(a) Healthy (b) Cordana

(c) Pestalotiopsis (d) Sigatoka

Figure 8: System testing results

From the figures above, it can be observed that the system implementation, along with the creation of the interface in MATLAB, is functioning properly. In the four tests conducted, no errors in the system or classification were encountered.

# 5 Conclusion

Based on the research conducted, the segmentation process to distinguish the area of banana leaf infected with the disease was successfully executed using the $A$ component in the LAB color space, with a threshold method applied at a threshold value of 0. Furthermore, the classification results using the Random Forest method demonstrated excellent performance, achieving an accuracy rate of 94.75%, with precision, recall, and F1-score values of 94.37%, 93.41%, and 93.89%, respectively. This high accuracy was attained through the fusion of information from the LAB color features and area features in both segmentation results, which included the segmentation of infected and uninfected areas.

Nevertheless, several limitations must be acknowledged. The dataset used consists of 1015 images and does not include data augmentation, which means the model's generalization ability under real-world conditions still requires further evaluation. Therefore, future research is encouraged to expand the data variation and apply augmentation techniques to enhance the model's robustness. In addition, Random Forest parameters such as the number of trees (50) and MaxNumSplits (100) were selected empirically based on initial trials and could be further optimized through hyperparameter tuning techniques such as grid search and random search. Moreover, incorporating additional features such as texture or spot shape could further improve classification accuracy, particularly in distinguishing diseases with visually similar symptoms.

The current system is developed in MATLAB and features a user interface that enables easy image loading, segmentation, and classification. While effective as an initial prototype, future development could involve migrating the system to the Python programming language for greater flexibility and integration capabilities. Additionally, adapting the system into an Android platform would enhance portability and usability on mobile devices for real-time field applications.

## References

[1] D. Šimoníková, J. Čížková, V. Zoulová, P. Christelová, and E. Hřibová, "Advances in the molecular cytogenetics of bananas, family musaceae," *Plants*, vol. 11, no. 4, p. 482, 2022, doi: https://doi.org/10.3390/plants11040482.

[2] Food and Agriculture Organization of the United Nations, "Food outlook: Biannual report on global food markets," Food and Agriculture Organization of the United Nations, Tech. Rep., 2019. [Online]. Available: http://www.fao.org/3/ca6911en/ca6911en.pdf

[3] Food and Agriculture Organization of the United Nations, "Agricultural production statistics 2000–2022," Tech. Rep., 2023. [Online]. Available: https://www.fao.org/3/cc9205en/cc9205en.pdf

[4] Food and Agriculture Organization of the United Nations, "Banana statistical compendium 2021," FAO, Tech. Rep., 2022. [Online]. Available: https://agfstorage.blob.core.windows.net/misc/FP_com/2022/10/12/Apo.pdf

[5] L. Tripathi, V. O. Ntui, and J. N. Tripathi, "Application of genetic modification and genome editing for developing climate-smart banana," *Food and Energy Security*, vol. 8, no. 4, pp. 1–16, 2019, doi: https://doi.org/10.1002/fes3.168.

[6] F. Dwivany, K. Wikantika, A. Sutanto, F. Ghazali, C. Lim, and G. Kamalesha, *Pisang Indonesia*. Bandung: ITB Press, 2021. [Online]. Available: https://www.researchgate.net/publication/350104189_PISANG_INDONESIA

[7] F. P. Castelan, L. A. Saraiva, F. Lange, L. De Lapeyre De Bellaire, B. R. Cordenunsi, and M. Chillet, "Effects of black leaf streak disease and sigatoka disease on fruit quality and maturation process of bananas produced in the subtropical conditions of southern brazil," *Crop Protection*, vol. 35, pp. 127–131, 2012, doi: https://doi.org/10.1016/j.cropro.2011.08.002.

[8] D. H. Marín, R. A. Romero, M. Guzmán, and T. B. Sutton, "Black sigatoka: An increasing threat to banana cultivation," *Plant Disease*, vol. 87, no. 3, pp. 208–222, 2003, doi: https://doi.org/10.1094/PDIS.2003.87.3.208.

[9] M. A. B. Bhuiyan, H. M. Abdullah, S. E. Arman, S. S. Rahman, and K. Al Mahmud, "Bananasqueezenet: A very fast, lightweight convolutional neural network for the diagnosis of three prominent banana leaf diseases," *Smart Agricultural Technology*, vol. 4, pp. 1–8, 2023, doi: https://doi.org/10.1016/j.atech.2023.100214.

[10] A. K. Singh, S. Sreenivasu, U. S. B. K. Mahalaxmi, H. Sharma, D. D. Patil, and E. Asenso, "Retracted: Hybrid feature-based disease detection in plant leaf using convolutional neural network, bayesian optimized svm, and random forest classifier," *Journal of Food Quality*, vol. 2024, pp. 1–16, Jan. 2024, doi: https://doi.org/10.1155/2024/9890349.

[11] P. Sahu, A. P. Singh, A. Chug, and D. Singh, "A systematic literature review of machine learning techniques deployed in agriculture: A case study of banana crop," *IEEE Access*, vol. 10, pp. 87 333–87 360, Aug. 2022, doi: https://doi.org/10.1109/ACCESS.2022.3199926.

[12] S. I. Guslianto, "Klasifikasi kematangan buah sawit berdasarkan fitur warna, bentuk dan tekstur menggunakan algoritma k-nn," *JEPIN: Jurnal Edukasi dan Penelitian Informatika*, vol. 9, no. 3, pp. 407–414, Dec. 2023, doi: https://doi.org/10.26418/jp.v9i3.64877.

[13] M. Y. Pusadan, I. Safitri, and Wirdayanti, "The image extraction using the hsv method to determine the maturity level of palm oil fruit with the k-nearest neighbor algorithm," *Jurnal RESTI*, vol. 7, no. 6, pp. 1448–1456, Dec. 2023, doi: https://doi.org/10.29207/resti.v7i6.5558.

[14] A. D. W. Sumari, P. I. Mawarni, and A. R. Syulistyo, "Classification of the quality quail eggs based on color and texture using k-nearest neighbor method and information fusion," *Jurnal Teknologi Informasi dan Ilmu Komputer*, vol. 8, no. 5, pp. 1019–1028, Oct. 2021, doi: https://doi.org/10.25126/jtiik.2021854393.

[15] N. M. Trieu and N. T. Thinh, "Using random forest algorithm to grading mango's quality based on external features extracted from captured images," *Journal of Image and Graphics*, vol. 11, no. 4, Dec. 2023, doi: https://doi.org/10.18178/joig.11.4.391-396.

[16] K. Saminathan, B. Sowmiya, and D. M. Chithra, "Multiclass classification of paddy leaf diseases using random forest classifier," *Journal of Image and Graphics*, vol. 11, no. 2, Jun. 2023, doi: https://doi.org/10.18178/joig.11.2.195-203.

[17] V. Chaudhari and M. Patil, "Banana leaf disease detection using k-means clustering and feature extraction techniques," in *International Conference on Advances in Computing, Communication and Materials*, Dehradun, India, Nov. 2020, pp. 126–130, doi: https://doi.org/10.1109/ICACCM50413.2020.9212816.

[18] V. V. Chaudhari and M. P. Patil, "Identification of banana disease using color and texture feature," in *Recent Trends in Image Processing and Pattern Recognition*. Singapore: Springer, Feb. 2021, pp. 238–248, doi: https://doi.org/10.1007/978-981-16-0493-5_21.

[19] N. S. M. Said, H. Madzin, S. K. Ali, and N. S. Beng, "Comparison of color-based feature extraction methods in banana leaf diseases classification using svm and k-nn," *Indonesian Journal of Electrical Engineering and Computer Science*, vol. 24, no. 3, pp. 1523–1533, Dec. 2021, doi: https://doi.org/10.11591/ijeecs.v24.i3.pp1523-1533.

[20] A. Ridhovan, A. Suharso, and C. Rozikin, "Disease detection in banana leaf plants using densenet and inception method," *Jurnal RESTI*, vol. 6, no. 5, pp. 710–718, Oct. 2022, doi: https://doi.org/10.29207/resti.v6i5.4202.

[21] R. Sangeetha, J. Logeshwaran, J. Rocher, and J. Lloret, "An improved agro deep learning model for detection of panama wilts disease in banana leaves," *AgriEngineering*, vol. 5, no. 2, pp. 660–679, Mar. 2023, doi: https://doi.org/10.3390/agriengineering5020042.

[22] L. Hakim, S. P. Kristanto, D. Yusuf, M. N. Shodiq, and W. A. Setiawan, "Disease detection of dragon fruit stem based on the combined features of color and texture," *INTENSIF: Jurnal Ilmiah Penelitian dan Penerapan Teknologi Sistem Informasi*, vol. 5, no. 2, pp. 161–175, Aug. 2021, doi: https://doi.org/10.29407/intensif.v5i2.15287.

[23] S. E. Arman, M. A. B. Bhuiyan, H. M. Abdullah, S. Islam, T. T. Chowdhury, and M. A. Hossain, "Bananalsd: A banana leaf images dataset for classification of banana leaf diseases using machine learning," *Data in Brief*, vol. 50, pp. 1–13, Oct. 2023, doi: https://doi.org/10.1016/j.dib.2023.109608.

[24] S. E. Arman, "Banana leaf spot diseases (bananalsd) dataset for classification of banana leaf diseases using machine learning," Jul. 2023, doi: https://doi.org/10.17632/9tb7k297ff.1.

[25] S. Kapadnis, "Banana disease recognition dataset," 2024, accessed: 2024-03-22. [Online]. Available: https://www.kaggle.com/datasets/sujaykapadnis/banana-disease-recognition-dataset

[26] Wulandari, Sasmita, M. R. Mulia, A. B. Kaswar, D. D. Andayani, and A. S. Agung, "Klasifikasi kandungan nutrisi buah pisang berdasarkan fitur tekstur dan warna lab menggunakan jaringan syaraf tiruan berbasis pengolahan citra digital," *Jurnal Teknologi Informasi dan Ilmu Komputer*, vol. 11, no. 3, pp. 507–518, Jul. 2024, doi: https://doi.org/10.25126/jtiik.938332.

[27] K. Anwar and S. Setyowibowo, "Segmentasi kerusakan daun padi pada citra digital," *JEPIN (Jurnal Edukasi dan Penelitian Informatika)*, vol. 7, no. 1, pp. 39–43, Apr. 2021, doi: https://doi.org/10.26418/jp.v7i1.42331.

[28] F. T. Anggraeny, M. S. Munir, and U. W. Atmojo, "Segmentasi k-means clustering pada citra warna daun tunggal menggunakan model warna l*a*b," *SCAN: Jurnal Teknologi Informasi dan Komunikasi*, vol. 14, no. 2, pp. 38–44, Jun. 2019, doi: https://doi.org/10.33005/scan.v14i2.1485.

[29] A. Premana, R. M. H. Bhakti, and D. Prayogi, "Segmentasi k-means clustering pada citra menggunakan ekstrasi fitur warna dan tekstur," *Jurnal Ilmiah Intech Information Technology Journal UMUS*, vol. 2, no. 1, pp. 89–97, May 2020, doi: https://doi.org/10.46772/intech.v2i01.190.

[30] M. Afriansyah, J. Saputra, V. Y. P. Ardhana, and Y. Sa'adati, "Algoritma naive bayes yang efisien untuk klasifikasi buah pisang raja berdasarkan fitur warna," *Journal of Information Systems Management and Digital Business*, vol. 1, no. 2, pp. 236–248, Jan. 2024, doi: https://doi.org/10.59407/jismdb.v1i2.438.

[31] Wulandari, D. F. Surianto, J. M. Parenreng, and F. Adiba, "Digital image based dss for assessing tomato quality using ahp-topsis method," *Digital Zone: Jurnal Teknologi Informasi dan Komunikasi*, vol. 15, no. 2, pp. 118–132, Nov. 2024, doi: https://doi.org/10.31849/digitalzone.v15i2.19060.

[32] A. D. W. Sumari, A. A. Alfian, and C. Rahmad, "Selection of quality coconut meat based on color and texture for quality wingko production using support vector machine (svm) and information fusion," *Jurnal Teknologi Informasi dan Ilmu Komputer*, vol. 8, no. 3, pp. 587–594, Jun. 2021, doi: https://doi.org/10.25126/jtiik.2021834391.

[33] A. Alofi, "A review of data fusion techniques," *International Journal of Computer Applications*, vol. 167, no. 7, pp. 37–41, Jun. 2017, doi: https://doi.org/10.5120/ijca2017914318.

[34] Y. O. Ouma, A. Keitsile, B. Nkwae, P. Odirile, D. Moalafhi, and J. Qi, "Urban land-use classification using machine learning classifiers: comparative evaluation and post-classification multi-feature fusion approach," *European Journal of Remote Sensing*, vol. 56, no. 1, pp. 291–312, Aug. 2023, doi: https://doi.org/10.1080/22797254.2023.2173659.

[35] T. M. Oshiro, P. S. Perez, and J. A. Baranauskas, "How many trees in a random forest?" in *Lecture Notes in Computer Science*. Berlin, Heidelberg: Springer, 2012, pp. 154–168, doi: https://doi.org/10.1007/978-3-642-31537-4_13.

[36] M. Grandini, E. Bagli, and G. Visani, "Metrics for multi-class classification: an overview," *arXiv preprint arXiv:2008.05756*, pp. 1–17, Aug. 2020, doi: https://doi.org/10.48550/arXiv.2008.05756.